

Journal of Materials Chemistry A

Accepted Manuscript

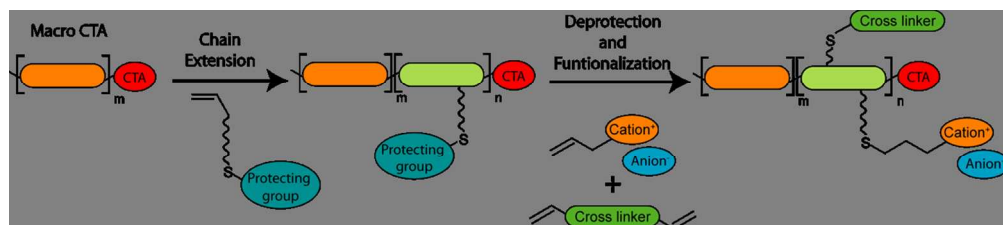


This is an *Accepted Manuscript*, which has been through the Royal Society of Chemistry peer review process and has been accepted for publication.

Accepted Manuscripts are published online shortly after acceptance, before technical editing, formatting and proof reading. Using this free service, authors can make their results available to the community, in citable form, before we publish the edited article. We will replace this *Accepted Manuscript* with the edited and formatted *Advance Article* as soon as it is available.

You can find more information about *Accepted Manuscripts* in the [Information for Authors](#).

Please note that technical editing may introduce minor changes to the text and/or graphics, which may alter content. The journal's standard [Terms & Conditions](#) and the [Ethical guidelines](#) still apply. In no event shall the Royal Society of Chemistry be held responsible for any errors or omissions in this *Accepted Manuscript* or any consequences arising from the use of any information it contains.



Robust and Orthogonal Approach to Access Modular Block-Copolymers Poly(ionic liquid)s

Modular Polymerized Ionic Liquid Block Copolymer Membranes for CO₂/N₂ Separation

Cite this: DOI: 10.1039/x0xx00000x

Brian J. Adzima,^a Surendar R Venna,^a Steven S. Klara,^b Hongkun He,^c Mingjiang Zhong,^c David R. Luebke,^a Meagan S. Mauter,^{*b} Krzysztof Matyjaszewski,^{*c} and Hunaid B. Nulwala^{*a,c}

Received 00th January 2012,
Accepted 00th January 2012

DOI: 10.1039/x0xx00000x

www.rsc.org/

The continuing discovery of broad classes of materials; such as ionic liquids, zeolites, metal organic frameworks, and block copolymers, present an enormous opportunity in developing materials for new applications. Polymerized ionic liquid block copolymers (PIL-BCPs) fall at the union of two already large sets of materials, and are emerging as a class of materials useful in gas separation membranes, ion and electron conducting materials, and as mechanical actuators. A wide range of ionic liquid moieties are possible as pendant groups along the polymer back, potentially allowing for wide variation in the resulting material properties; however in practice the range of ionic liquids explored is hindered by the need to optimize polymerization conditions for each new monomer. Here, we present a modular approach to PIL-BCP synthesis where a variety of olefin bearing cations are readily conjugated to polymers using thiol-Michael click chemistry. This approach allowed for the rapid development of a diverse materials library including phase separated thin films, ion-gels, and liquid PIL-BCPs, with a reduced investment in synthetic time. Finally, we demonstrate that this approach identified PIL-BCPs with increased CO₂ permeability relative to PILs, which could find use in carbon capture from flue gas.

INTRODUCTION

Ionic liquids (ILs) are an emerging class of solvent with unique solubility and conductive properties. The liquid nature of these technologically important materials makes it difficult to incorporate them in device oriented applications such as proton switchable surfaces,¹ electron and ion conductors,²⁻⁶ gas separation membranes,^{7,8} sensors,⁹ and actuators.¹⁰ Poly(ionic liquid)s (PILs) have been investigated as solid-state alternatives that confer processing advantages over ILs.¹¹⁻¹⁴ PILs are generally solid materials with lower glass transition temperatures (T_g) than ILs, and certain properties are reduced as a result of the solid nature of PILs. For instance, the gas permeance and conductivity of PILs are typically reduced compared to their equivalent ILs.¹⁵ As a result of their lower T_g , PILs tend to be gels which are difficult to process into the thin films needed in many applications.

PIL-based block copolymers (PIL-BCPs) offer a second approach that balances processability with functionality. In PIL-BCPs, low and high T_g segments phase separate at nanometer scale. If designed properly, ionic domains with low T_g can be used to provide efficient transport of ions, electrons, or gas, while a second domain provides structural integrity.¹⁶ It

has also been proposed that diffusivity can be increased by reducing the dimensionality of overall ion diffusion.¹⁷ The reduction in dimensionality can also lead to nanoconfinement, which has been shown to increase mobility and diffusion of gas molecules.¹⁸

The major chemical functionality factors influencing the properties of PIL-BCPs are the polymer backbone, anion, cation, arrangement, block length, and topology.^{11,19,20} Given these six factors, the design space for PIL-BCPs is broad, and the potential to tailor the materials to specific applications is high. Specially, PIL-BCP materials can form the good gas separation membranes and have the potential to show high separation performances. There is always trade-off exists between CO₂ permeability and CO₂/N₂ selectivity of the present membranes such as polyimides, polysulfones, polyelectrolytes etc. and materials with high gas separation performance above the Robeson upper bound are exceptionally rare.²¹⁻²³ The transport of gases in dense nonporous polymers follows the solution-diffusion mechanism and it was reported that diffusivity plays the critical role in achieving the high selectivity compared to gas solubility.²⁴ It is easy to fine tune these PIL-BCPs materials compared to conventional polymer

membranes by changing above mentioned functionalities in order to enhance the diffusivity and/or solubility and hence able to achieve permeability and selectivity above the Robeson upper bound.

EXPERIMENTAL SECTION

Materials:

All chemicals were purchased from Acros Organics, TCI America, or Sigma Aldrich and used as received, unless otherwise noted. ^1H NMR spectra were recorded in CDCl_3 on a Bruker Avance III 500 spectrometer. A TA Instruments Q2000 DSC equipped with liquid nitrogen cooling accessory was used to measure the glass transition temperature. The midpoint value of the glass transition was reported after three heating and cooling cycles at $20\text{ }^\circ\text{C}/\text{min}$ under N_2 protection. Three samples were averaged and the standard error reported.

Synthesis details are included in the supporting information.

AFM information:

Tapping mode atomic force microscopy (TMAFM) studies were carried out with the aid of a NanoScope III-M system (Digital Instruments, Santa Barbara, CA), equipped with a J-type vertical engage scanner. The AFM observations were performed at room temperature under air using silicon cantilevers with spring constant of 20 - 80 N/m and nominal resonance frequency of 230-410 kHz (Tapping Mode Etched Silicon Probes).

Small and Wide Angle X-Ray Scattering:

All SAXS and WAXS measurements were performed on a Rigaku instrument, model MSA BS0187 at a wavelength of 0.15405 nm. SAXS measurements were recorded with an electronic detector at a distance of 1786.27 mm. WAXS measurements were recorded on a Fuji Image Plate at a distance of 72.5 mm. All analysis was completed with SAXS GUI software. Detail WAXS and SAXS data can be found in supporting information.

Gel permeation chromatography (GPC):

Molecular weight and molecular weight distribution (Mw/Mn) values were determined by GPC. The GPC measurement was performed with a Waters 515 HPLC pump and a Waters 2414 refractive index detector using PSS columns (Styrogel 102, 103, 105 Å) in tetrahydrofuran (THF) as an eluent at a flow rate of 1 mL/min at $35\text{ }^\circ\text{C}$.

Measurement of gas separation performance:

The single-component CO_2 and N_2 permeation tests were performed at room temperature using the isochoric (constant volume, variable-pressure) permeation system. All gasses used in this study were Dry-UHP grade gasses from Butler Gas Company. Schematic of this unit is shown in S-Figure 1. Upstream pressures were measured with a pressure transducer

(Maximum pressure 150 psia, viatran Inc., Model-345) and accompanying readout (Dalec electronics digital panel). Downstream pressures were measured using a Baratron® 627D capacitance manometer with a maximum pressure output of 10 Torr (MKS, Wilmington, MA). The downstream volume in Figure 1 is calibrated by using a simple mole balance using a known volume of stainless steel balls. The thicknesses of the membranes were measured using a micrometer (Marathon Electronic digital micrometer) several times and their average value was used for analysis.

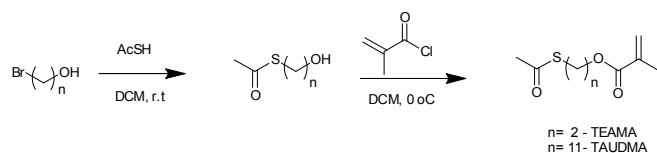
RESULTS AND DISCUSSION

To access PIL-block copolymers (BCPs), two main strategies are generally utilized: the polymerization of non-ionic monomers followed by subsequent modification;^{15,16,25–28} and the direct polymerization of functionalized ILs.^{29–33} The former allows the use of conventional gel permeation chromatography for characterization of molecular weights—a key tool for developing well controlled polymerizations. The latter ensures complete functionalization but can require special techniques for molecular weight measurements.^{28,30,32} *N*-Vinyl imidazoles and their derivatives are even more challenging,^{34,35} and polymers with broad molecular weight distributions may be produced under conditions which are effective for other reactions.³⁶

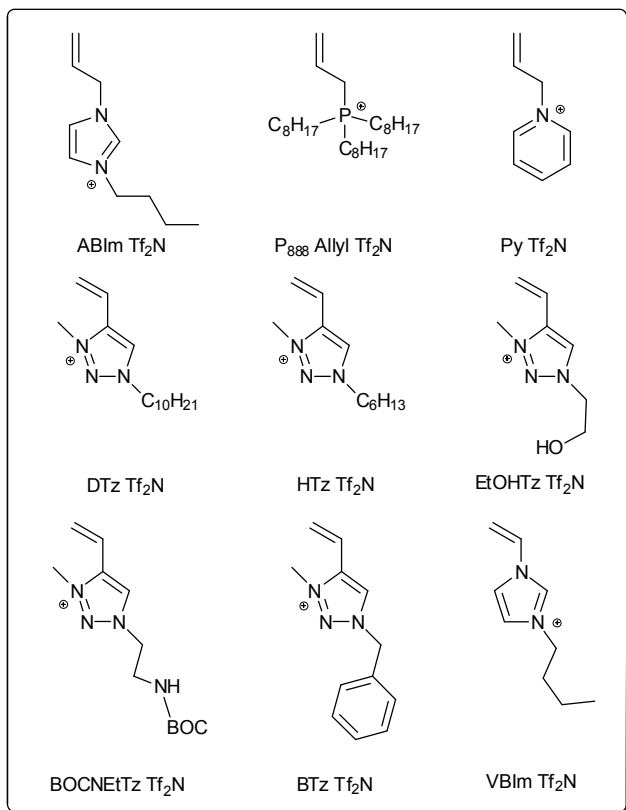
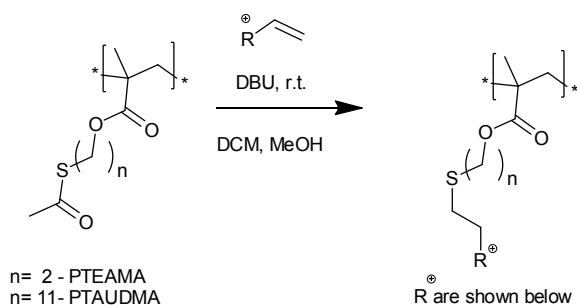
These problems cause the rate determining step for new material development to become the identification of polymerization conditions for each new IL monomer. A more efficient approach is to first prepare a common BCP, and then conjugate it with a wide variety of ionic liquids. Activated esters have been used for this purpose;³⁷ however, click chemistry offers a number of more atom-efficient reactions.^{38–41} The copper-catalyzed azide–alkyne cycloaddition (CuAAC) is an obvious choice, but azides and alkynes have limited reactivity outside the CuAAC reaction. Thus in this application, functional group tolerance limits the development of a modular reaction. Alternatively, thiols react with a wide range of functional groups: alkenes (electronically activated, electronically deactivated, and strained), epoxies, alkynes, halides, isocyanates, and thiols.^{42–47} Using a protecting group, thiol functionalized monomers can be polymerized using reversible addition-fragmentation chain transfer (RAFT) polymerization.^{48,49}

(Meth)acrylate based monomers bearing thioacetate groups were synthesized as shown in Scheme 1. These monomers underwent free radical, RAFT, and (co)polymerization reactions using generic conditions. Chain extension from poly(methyl methacrylate) (PMMA) using cumyl and poly(propylene glycol) was performed using dithiobenzoate based macro chain transfer agents. The resulting polymers have glass transition temperatures between -49 and $102\text{ }^\circ\text{C}$. PTAUMAD was exclusively used in further experiments. Removal of the protecting group and a simultaneous thio-Michael reaction was accomplished by using 1,8-

diazabicycloundec-7-ene (DBU) as a catalyst (Scheme 2). This reaction was quantitative with small molecule analogues.



Scheme 1. Synthesis scheme for protected (meth)acrylate monomers.



Scheme 2. Simultaneous de-protection and thio-Michael addition. (Box) Vinyl and allyl functionalized ionic liquids used in this study for simultaneous de-protection and coupling.

Bis(trifluoromethane)sulfonamide Tf_2N is the common anion in this study. **VBIm** Tf_2N and **Py** Tf_2N were not amenable to scheme 2.

The simultaneous de-protection and coupling strategy was found to readily translate to seven of the nine ionic liquids tested. Allyl functionalized imidazolium and phosphonium bis(trifluoromethylsulfonamide) (AIm Tf_2N and P_{888} allyl Tf_2N) ionic liquids, as well as a series of 4-vinyl triazolium^{50,51} species, were readily conjugated to PMMA-*b*-PTAUMAD. 1-Vinyl pyridinium Tf_2N underwent an unknown side reaction with DBU and 1-vinyl imidazolium Tf_2N proved entirely unreactive, perhaps due to electron-donation from the imidazolium ring. Conversion, as determined by ^1H NMR was less than quantitative, likely due to steric hindrance (see supporting information).

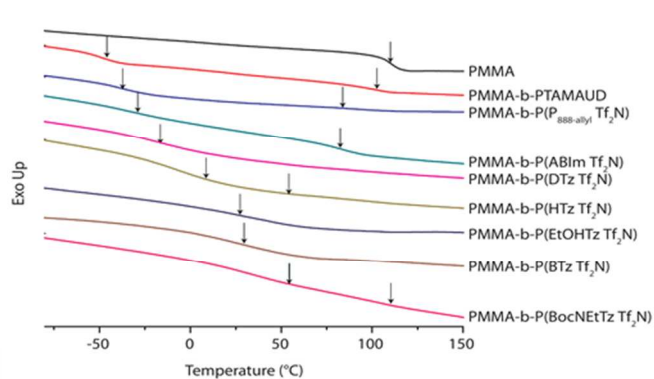


Figure 1. DSC thermograms with black arrows indicating the midpoint of the glass transition temperatures for PMMA-*b*-PILs

Low T_g s have been associated with high gas solubility and conductivity in PILs,^{6,15,52} so differential scanning calorimetry (DSC) was used to both measure the T_g and screen for phase separation (**Figure 1**). T_g s were found to be in the range of -40 to 50 °C for the materials. Several PILs showed a second glass transition temperature over 80 °C, indicating phase separation. Phase separation was confirmed by small-angle X-ray scattering (SAXS, Figure 2) and atomic force microscopy (Figure 3b). The lack of phase separation in some of the PIL-BCPs is surprising. BCPs and polymer blends of sulfonated polystyrene and styrene have effective Flory-Huggins interaction parameters an order of magnitude greater than between non-charged polymers.^{53–55} However, other researchers have also noted weak microphase separation in PMMA-*b*-PILs.²⁷ This phenomenon is likely not due to incomplete functionalization, we suspect it is due to the existence of co-continuous morphologies.⁵⁶

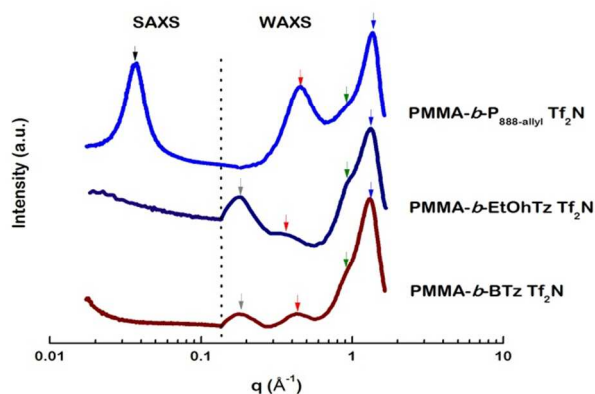


Figure 2. SAXS and WAXS profiles of three PILs

We performed X-ray scattering on three of the eight PILs samples: PMMA-*b*-P_{888-allyl}Tf₂N, PMMA-*b*-EtOhTz Tf₂N, and PMMA-*b*-BTz Tf₂N. SAXS characterizes microphase separation and other structural features in the low *q*-range (Figure 2, black arrow), where *q* refers to the scattering vector. Only the PMMA-*b*-P_{888-allyl}Tf₂N PIL scatters in the low *q*-range (*d*-spacing 17.14 nm), which is consistent with the DSC results presented above. Large *q*-spacings measured in wide-angle X-ray scattering (WAXS) measurements are useful for determining the structure and spacing of the polymer backbone and side chains. The PMMA-*b*-EtOhTz Tf₂N, and PMMA-*b*-BTz Tf₂N PIL-BCPs display multiplet-cluster peaks with *d*-spacings of 3.63 and 3.57 nm, respectively (Figure 2, grey arrows).⁵⁷ All three samples displayed a peak with a *d*-spacing between 1.3 nm and 1.8 nm, which we believe to be the PMMA backbone-to-backbone spacing distance (Figure 2, red arrows). A small shoulder peak on each sample with *d*-spacings between 0.65 nm and 0.67 nm represents the anion-to-anion distances within each polymer (Figure 2, green arrows).⁵⁸ And a large peak present on each sample at a *d*-spacing between 0.45 and 0.48 nm corresponds to the distance between PIL side chains (blue arrows). These peak assignments agree favorably with previous literature.⁵⁹ Side chain ordering in cast films appears to be higher than in powders, which may be due to ordering during the solvent evaporation process (see Supporting Information Figure 2).

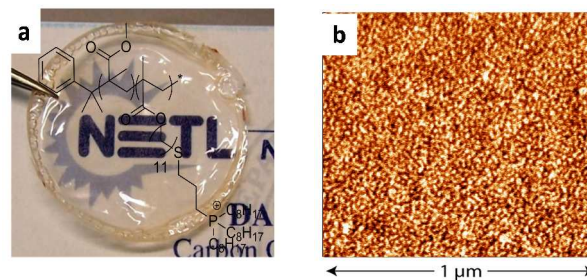


Figure 3. a) Free standing membrane of PMMA-*b*-P(P_{888-allyl}Tf₂N) b) AFM phase image of the above film showing microphase separation.

The facile synthesis of PIL-BCPs allowed us to screen the above BCP for gas separation membrane materials. In addition to evaluating the brittleness and casting potential of each material, we also evaluated the permeability (*P*), which relates the mass flux across the membrane (*M*), pressure difference across the membrane (ΔP) and the membrane thickness (*l*);

$$P = (M \cdot l) / \Delta P \quad \text{Equation (1)}$$

The ability of a membrane to separate two gases can be described by the ideal selectivity (α);

$$\alpha_{ideal} = P_a / P_b \quad \text{Equation (2)}$$

CO₂/N₂ gas separation performance measurements, showed that the PMMA-*b*-P(P_{888-allyl}Tf₂N) membrane (Figure 3a) had a CO₂ permeability of 71 Barrer, and a CO₂/N₂ selectivity of 20. However, the non-phase separated PMMA-*b*-P(BVTz Tf₂N) had a CO₂ permeability of 24 Barrer. Interestingly, the two ILs had similar glass transition temperatures (-50 °C for P_{888-allyl}Tf₂N and -58 °C for BVTz Tf₂N). Thus, it seems that the presence of phase separation in PMMA-*b*-P_{888-allyl}Tf₂N increases CO₂ permeability. Experiments in other PIL-BCPs have given similar indications.

The PMMA-*b*-P(P_{888-allyl}Tf₂N) shows greater permeability than PILs reported in the literature (Figure 4). Compared to ion-gels and IL-PIL composites, the permeability of our non-optimized materials is lower; however, it should be noted that the ability to cast thinner films of PIL-BCPs may allow higher permeance (*P/l*) films to be prepared on a porous support layer. As the phase separation as well as ideal IL-block in these materials remains to be optimized, further increases in permeability and selectivity are likely. Preparation of membranes with a sufficiently high permeance (*P/l*, greater than 1000 GPU) to enable economical capture of CO₂ from flue gas is a challenge that remains to be met.

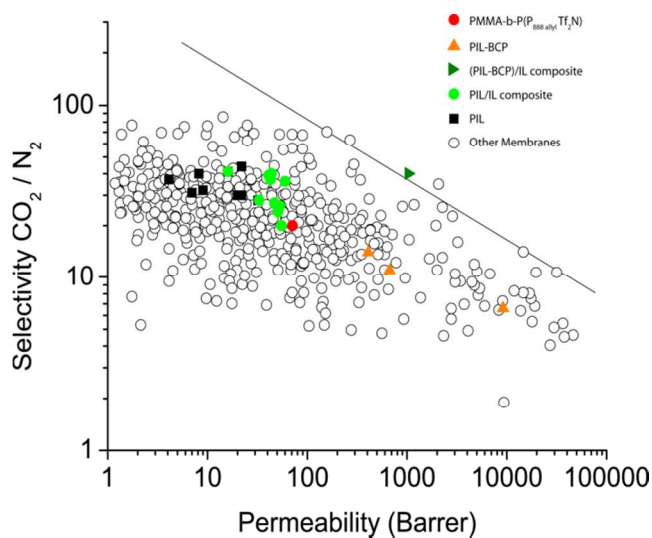


Figure 4. Robeson plot comparing PILs, PIL-IL composites, ion gels, and PIL-BCPs.^{7,15,16,21,60–63}

Conclusions

In conclusion, BCPs with pendant thioacetates can be used to efficiently prepare PIL-BCPs with a wide range of pendant ILs including phosphonium, triazolium, and imidazolium cations. This approach can likely be extended to other than ionic liquids, and perhaps even to those functionalized with other thiol-reactive groups (e.g., epoxies). The PIL-containing BCPs prepared by this approach showed a wide range of glass transition temperatures, and many were phase separated. Finally, when phase separated, these materials show increased permeability relative to PILs while maintain CO_2/N_2 selectivity. This result suggests PIL-containing BCPs could be useful materials for the economical capture of CO_2 from flue gas emissions.

Acknowledgements

This technical effort was also performed in support of U.S. Department of Energy's National Energy Technology Laboratory's on-going research on CO_2 capture under the contract DE-FE0004000.

DISCLAIMER

This project was funded by the Department of Energy, National Energy Technology Laboratory, an agency of the United States Government, through a support contract with URS Energy & Construction, Inc. Neither the United States Government nor any agency thereof, nor any of their employees, nor URS Energy & Construction, Inc., nor any of their employees, makes any warranty, expressed or implied, or assumes any legal liability or responsibility for the accuracy, completeness, or usefulness of any information, apparatus, product, or process disclosed, or represents that its use would not infringe privately owned rights. Reference herein to any specific commercial

product, process, or service by trade name, trademark, manufacturer, or otherwise, does not necessarily constitute or imply its endorsement, recommendation, or favoring by the United States Government or any agency thereof. The views and opinions of authors expressed herein do not necessarily state or reflect those of the United States Government or any agency thereof.

Notes and references

^a National Energy Technology Laboratory, Pittsburgh, PA 15236

^b Department of Chemical Engineering, Carnegie Mellon University, 5000 Forbes Avenue, Pittsburgh, PA 15213. mauter@cmu.edu

^c Department of Chemistry, Carnegie Mellon University, 4400 Fifth Avenue, Pittsburgh, PA 15213. km3@andrew.cmu.edu; hnulwala@andrew.cmu.edu

Electronic Supplementary Information (ESI) available: [Testing protocols, Synthetic protocols, characterisations]. See DOI: 10.1039/b000000x/

1. S. Long, F. Wan, W. Yang, H. Guo, X. He, J. Ren, and J. Gao, *J. Appl. Polym. Sci.*, 2013, **128**, 2687–2693.
2. H. Ohno, M. Yoshizawa, and W. Ogihara, *Electrochim. Acta*, 2004, **50**, 255–261.
3. M. Li, L. Yang, S. Fang, S. Dong, S. Hirano, and K. Tachibana, *Polym. Int.*, 2012, **61**, 259–264.
4. M. Li, L. Yang, S. Fang, and S. Dong, *J. Memb. Sci.*, 2011, **366**, 245–250.
5. H. Chen, J.-H. Choi, D. Salas-de la Cruz, K. I. Winey, and Y. A. Elabd, *Macromolecules*, 2009, **42**, 4809–4816.
6. M. D. Green, D. Salas-de la Cruz, Y. Ye, J. M. Layman, Y. A. Elabd, K. I. Winey, and T. E. Long, *Macromol. Chem. Phys.*, 2011, **212**, 2522–2528.
7. J. E. Bara, S. Lessmann, C. J. Gabriel, E. S. Hatakeyama, R. D. Noble, and D. L. Gin, *Ind. Eng. Chem. Res.*, 2007, **46**, 5397–5404.
8. J. E. Bara, D. E. Camper, D. L. Gin, and R. D. Noble, *Acc. Chem. Res.*, 2010, **43**, 152–159.
9. Q. Zhao, M. Yin, A. P. Zhang, S. Prescher, M. Antonietti, and J. Yuan, *J. Am. Chem. Soc.*, 2013, **135**, 5549–52.
10. M. D. Green, D. Wang, S. T. Hemp, J.-H. Choi, K. I. Winey, J. R. Heflin, and T. E. Long, *Polymer (Guildf.)*, 2012, **53**, 3677–3686.
11. J. Yuan, D. Mecerreyes, and M. Antonietti, *Prog. Polym. Sci.*, 2013, **38**, 1009–1036.
12. J. Yuan and M. Antonietti, *Polymer (Guildf.)*, 2011, **52**, 1469–1482.
13. J. Yuan, S. Soll, M. Drechsler, A. H. E. Müller, and M. Antonietti, *J. Am. Chem. Soc.*, 2011, **133**, 17556–9.

14. H. He, B. Adzima, M. Zhong, S. Averick, R. Koepsel, H. Murata, A. Russell, D. Luebke, A. Takahara, H. Nulwala, and K. Matyjaszewski, *Polym. Chem.*, 2014.
15. Y. Gu and T. P. Lodge, *Macromolecules*, 2011, **44**, 1732–1736.
16. P. T. Nguyen, E. F. Wiesenauer, D. L. Gin, and R. D. Noble, *J. Memb. Sci.*, 2013, **430**, 312–320.
17. D. Sidebottom, *Phys. Rev. Lett.*, 1999, **83**, 983–986.
18. W. Shi and D. C. Sorescu, *J. Phys. Chem. B*, 2010, **114**, 15029–41.
19. D. Mecerreyes, *Prog. Polym. Sci.*, 2011, **36**, 1629–1648.
20. F. S. Bates, M. A. Hillmyer, T. P. Lodge, C. M. Bates, K. T. Delaney, and G. H. Fredrickson, *Science*, 2012, **336**, 434–40.
21. L. M. Robeson, *J. Memb. Sci.*, 2008, **320**, 390–400.
22. C. E. Powell and G. G. Qiao, *J. Memb. Sci.*, 2006, **279**, 1–49.
23. C. Lin, Q. Chen, S. Yi, M. Wang, and S. L. Regen, *Langmuir*, 2014, **30**, 687–91.
24. B. D. Freeman, *Macromolecules*, 1999, **32**, 375–380.
25. K. Vijayakrishna, S. K. Jewrajka, A. Ruiz, R. Marcilla, J. A. Pomposo, D. Mecerreyes, D. Taton, and Y. Gnanou, *Macromolecules*, 2008, **41**, 6299–6308.
26. K. Vijayakrishna, D. Mecerreyes, Y. Gnanou, and D. Taton, *Macromolecules*, 2009, **42**, 5167–5174.
27. Y. Ye, J.-H. Choi, K. I. Winey, and Y. A. Elabd, *Macromolecules*, 2012, **45**, 7027–7035.
28. H. Mori, Y. Ebina, R. Kambara, and K. Nakabayashi, *Polym. J.*, 2012, **44**, 550–560.
29. E. Karjalainen, N. Chenna, P. Laurinmäki, S. J. Butcher, and H. Tenhu, *Polym. Chem.*, 2013, **4**, 1014.
30. H. He, M. Zhong, B. Adzima, D. Luebke, H. Nulwala, and K. Matyjaszewski, *J. Am. Chem. Soc.*, 2013, **135**, 4227–4230.
31. S. Cheng, F. L. Beyer, B. D. Mather, R. B. Moore, and T. E. Long, *Macromolecules*, 2011, **44**, 6509–6517.
32. S. J. Ding, H. D. Tang, M. Radosz, and Y. Q. Shen, *J. Polym. Sci., Part A Polym. Chem.*, 2004, **42**, 5794–5801.
33. H. He, S. Averick, E. Roth, D. Luebke, H. Nulwala, and K. Matyjaszewski, *Polymer (Guildf.)*, 2014.
34. S. T. Hemp, M. Zhang, M. Tamami, and T. E. Long, *Polym. Chem.*, 2013, **4**, 3582.
35. M. H. Allen, S. T. Hemp, A. E. Smith, and T. E. Long, *Macromolecules*, 2012, **45**, 3669–3676.
36. H. Mori, M. Yahagi, and T. Endo, *Macromolecules*, 2009, **42**, 8082–8092.
37. Y. Schneider, M. A. Modestino, B. L. McCulloch, M. L. Hoarfrost, R. W. Hess, and R. A. Segalman, *Macromolecules*, 2013, **46**, 1543–1548.
38. H. C. Kolb, M. G. Finn, and K. B. Sharpless, *Angew. Chemie Int. Ed.*, 2001, **40**, 2004–2021.
39. W. H. Binder and R. Sachsenhofer, *Macromol. Rapid Commun.*, 2007, **28**, 15–54.
40. P. Dimitrov-Raytchev, S. Beghdadi, A. Serghei, and E. Drockenmuller, *J. Polym. Sci. Part A Polym. Chem.*, 2013, **51**, 34–38.
41. K. Takizawa, H. Nulwala, R. J. Thibault, P. Lowenhielm, K. Yoshinaga, K. L. Wooley, and C. J. Hawker, *J. Polym. Sci. Part A Polym. Chem.*, 2008, **46**, 2897–2912.
42. C. E. Hoyle, A. B. Lowe, and C. N. Bowman, *Chem. Soc. Rev.*, 2010, **39**, 1355–87.
43. B. J. Adzima and C. N. Bowman, *AIChE J.*, 2012, **58**, 2952–2965.
44. N. Cengiz, J. Rao, A. Sanyal, and A. Khan, *Chem. Commun. (Camb.)*, 2013, **49**, 11191–3.
45. I. Gadwal and A. Khan, *Polym. Chem.*, 2013, **4**, 2440.
46. S. De, C. Stelzer, and A. Khan, *Polym. Chem.*, 2012, **3**, 2342.
47. S. De and A. Khan, *Chem. Commun. (Camb.)*, 2012, **48**, 3130–2.
48. E. Hrsic, I. Zografou, B. Schulte, A. Pich, H. Keul, and M. Möller, *Polymer (Guildf.)*, 2013, **54**, 495–504.
49. R. Nicolaÿ, *Macromolecules*, 2012, **45**, 821–827.
50. H. B. Nulwala, C. N. Tang, B. W. Kail, K. Damodaran, P. Kaur, S. Wickramanayake, W. Shi, and D. R. Luebke, *Green Chem.*, 2011, **13**, 3345.
51. B. Adzima, S. C. Taylor, H. He, D. R. Luebke, K. Matyjaszewski, and H. B. Nulwala, *J. Polym. Sci. Part A Polym. Chem.*, 2013.
52. U. H. Choi, M. Lee, S. Wang, W. Liu, K. I. Winey, H. W. Gibson, and R. H. Colby, *Macromolecules*, 2012, **45**, 3974–3985.
53. N. C. B. Tan, X. Liu, R. M. Briber, and D. G. Peiffer, *Polymer (Guildf.)*, 1995, **36**, 1969–1973.
54. N. C. Zhou, C. Xu, W. R. Burghardt, R. J. Composto, and K. I. Winey, *Macromolecules*, 2006, **39**, 2373–2379.
55. M. J. Park and N. P. Balsara, *Macromolecules*, 2008, **41**, 3678–3687.
56. P. Knychala, M. Dziecielski, M. Banaszak, and N. P. Balsara, *Macromolecules*, 2013, **46**, 5724–5730.

Journal Name

ARTICLE

57. A. Eisenberg, B. Hird, and R. B. Moore, *Macromolecules*, 1990, **23**, 4098–4107.
58. K. Nakamura, T. Saiwaki, K. Fukao, and T. Inoue, *Macromolecules*, 2011, **44**, 7719–7726.
59. M. H. Allen, S. Wang, S. T. Hemp, Y. Chen, L. A. Madsen, K. I. Winey, and T. E. Long, *Macromolecules*, 2013, **46**, 3037–3045.
60. T. C. Merkel, H. Lin, X. Wei, and R. Baker, *J. Memb. Sci.*, 2010, **359**, 126–139.
61. P. Li, D. R. Paul, and T.-S. Chung, *Green Chem.*, 2012, **14**, 1052–1063.
62. Y. Gu, E. L. Cussler, and T. P. Lodge, *J. Memb. Sci.*, 2012, **423**, 20–26.
63. J. E. Bara, R. D. Noble, and D. L. Gin, *Ind. Eng. Chem. Res.*, 2009, **48**, 4607–4610.